ELSEVIER

Journal of Nuclear Materials 304 (2002) 15–20

journal of nuclear materials

www.elsevier.com/locate/jnucmat

Sputtering and ion-induced electron emission of graphite under high-dose nitrogen bombardment

A.M. Borisov [a,*], W. Eckstein [b], E.S. Mashkova [a]

[a] *Institute of Nuclear Physics, Moscow State University, 119992 Moscow, Russia*
[b] *Max-Planck-Institute fur Plasmaphysik, Boltzmannstr. 2, 85748 Garching, Germany*

Received 7 December 2001; accepted 20 April 2002

Abstract

The dependence of the sputtering yield Y and the electron emission coefficient γ of isotropic graphites (POCO-AXF-5Q and Russian MPG-LT) on ion fluence and ion incidence angle θ at near room temperatures and the dependence of γ on target temperature under high dose 30 keV N_2^+ ion irradiation were measured. It was found that Y and γ are stabilized at fluences $F \geqslant 1 \times 10^{19}$ N/cm^2. A specific target surface topography develops. At steady-state conditions, the N concentration in MPG-LT is 19 at.% and in POCO16 at.%. In the angular range $\theta = 0$–$80°$, Y and γ increase and the angular dependence of Y is slightly stronger than that of γ. Sputtering yields of POCO are 1.5 times higher than those of MPG-LT. The reasons of the difference between the experimental and calculated sputtering yields using the TRIM.SP code are discussed. The dependence of γ on the target temperature manifests a step-like increase at $\simeq$250 °C which may be due to radiation induced structure transformation in the modified surface layer. © 2002 Published by Elsevier Science B.V.

1. Introduction

The material problems of modern fusion devices are largely connected with the graphite behaviour under ion bombardment [1]. In the last years intensive studies of new materials preparation on the basis of carbon-nitride compounds were carried out, see for example [2–5]. In this connection the investigations of the regularities of high-dose nitrogen irradiation of carbon-based materials, namely, the regularities of ion-induced electron emission, sputtering, nitrogen depth profiles, and the development of the surface topography are of interest. Experimental data of nitrogen ion irradiation on graphites, in particular, of sputtering and ion-induced electron emission are scarce [4,6–8]. Computer simulation of graphite sputtering by nitrogen were obtained in the energy range from 10 to 1000 eV [9]. Recently, the simulated results of the dependence of graphite sputtering yields on ion incidence in a wide angular range at a nitrogen ion energy of 15 keV were published and compared with the experimental results [10].

It should be noted that the regularities of ion-induced electron emission were often used to analyse transitions in the surface layer modified by ion irradiation, both in order–disorder changes in semiconductors [11,12] and in transitions to steady-state conditions [13,14]. However, data even on basic integral characteristics of the ion-induced electron emission coefficient, γ, of graphites are not numerous.

The aim of this paper is to study the dependence of the sputtering yield, Y, and the ion-induced electron emission coefficient, γ, on irradiation fluence and the ion incidence angle, the dependence of γ on target temperature, the implanted nitrogen concentration and the developing surface topography for isotropic graphites under high-dose N_2^+ ion bombardment.

* Corresponding author. Tel.: +7-095 939 3904; fax: +7-095 939 0896.
E-mail address: borisov@anna19.npi.msu.su (A.M. Borisov).

0022-3115/02/$ - see front matter © 2002 Published by Elsevier Science B.V.
PII: S0022-3115(02)00871-1

2. Experimental

The experiment was performed using the mass-monochromator of the Institute of Nuclear Physics, Moscow State University [15]. The 5–35 keV ion beam was produced in an arc source with a longitudinal magnetic field. The ions were separated and the beam was focused by a Siegbahn-type magnetic sector field. The angular spread of the ion beam at the focus of the instrument was $\pm 1°$. The targets were mounted in the collision chamber; the schematic was presented in [16]. The target holder permitted the variation of the angle of ion incidence from 0° to 89° with an angular step of 0.25–0.5° and the variation of the target temperature from RT to 1000 °C. The samples used in this work were cut from massive pieces of isotropic graphites both of Russian-made graphite (NII Graphite, Moscow) MPG-LT with $\rho = 1.7$ g/cm^3 and US-produced graphite POCO-AXF-5Q with $\rho = 1.82$ g/cm^3. The sample thickness was 4 mm, the width 22 mm, and the length was chosen depending on the ion incidence angle from 30 to 80 mm. The samples were mechanically polished, washed in ethanol, annealed in vacuum as it was produced before Y measurements of MPG-LT graphite under Ar^+ ion irradiation [16]. Vacuum annealing of graphites was necessary due to the tendency of graphites to adsorb gases very intensively [17]. The target irradiation was carried out mainly with 30 keV N_2^+ ions. The working pressure during the irradiation process was better than 7×10^{-10} bar. The total ion current was 0.1–0.2 mA, the cross-section of the ion beam was 0.35 cm^2. Ion fluences (in scale of two atomic N particles) were 10^{18}–10^{19} N/cm^2. Sputtering yields were determined by weight loss measurements assuming molecular ion dissociation by interaction with the solid. The sensitivity of the weight measurement was 0.02 mg. The error of the measured yield, Y, was estimated to be 15%, mainly due to the necessity to take into account gas adsorption. The ion-induced electron emission coefficient, γ, was determined as the ratio of the electron current to the primary ion current. Before and after ion irradiation the samples were analysed by SEM and Rutherford backscattering spectrometry (RBS) using the 1.5–1.8 MeV $^4He^+$ beam of the Van de Graaff accelerator of the Institute of Nuclear Physics, Moscow State University. The RBS spectra were simulated using the NBS code [18].

3. Simulation

The simulation of the nitrogen interaction with graphite was produced using the program TRIM.SP (version trvmc) [19,20]. It should be reminded that TRIM.SP simulates only the low fluence or equilibrium case, when elemental composition and other parameters of an irradiated target do not change. A randomized target structure is assumed and the atomic interactions are treated as a sequence of binary collisions. In all calculations the WHB (Kr–C) potential [21] is applied. The inelastic energy loss is described by an equipartition of the continuous Lindhard–Scharff [22] and the local Oen–Robinson [23] models. The target density, ρ, is assumed to be 1.7, 1.85 and 2.26 g/cm^3 for a pure C target and $\rho = 1.85$ g/cm^3 for the target with a composition ratio of C:N:O = 77:19:4. The surface binding energy is chosen to be 7.4 eV (graphite sublimation energy). Particle statistics over bombarding particles is $(0.5–2) \times 10^6$ depending on the situation to be simulated.

4. Results and discussion

As it was pointed out above, the γ-dependence on the ion fluence may be used to control the transition dynamics of the irradiated target to steady-state conditions. In the present work it has been found, that the stabilization (steady-state) of γ with fluence occurs at $F \simeq 1 \times 10^{19}$ N/cm^2 practically at any chosen ion incidence angle. A typical example is presented in Fig. 1 [24]. Such fluences are also needed to stabilize sputtering yields. In particular at $\theta = 70°$, as the fluence increases Y rises, then passes a maximum and approaches a plateau, see Fig. 1. One may suppose that such a situation gives evidence of reaching steady-state conditions, when an amount of the implanted species remains constant; then the weight loss of the target is a measure of the sputtering yield of the target with a characteristic surface topography. All values of γ and Y presented below correspond to such steady-state conditions.

SEM studies have shown that the initial surface topography (the pores and the flakes between them, see Fig. 2(a)) is transformed after high-dose irradiation.

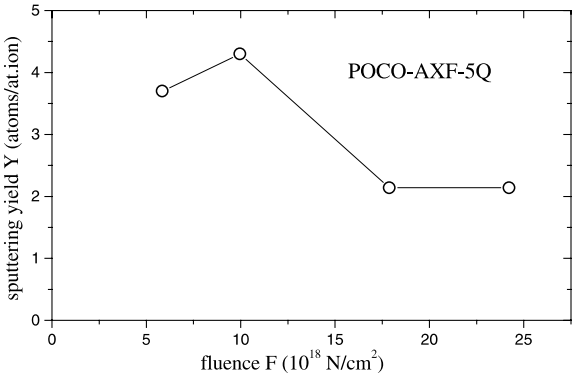

Fig. 1. The dependence of the sputtering yield, Y, on ion fluence F for POCO-AXF-5Q under 30 keV N_2^+ ion irradiation at $\theta = 70°$ (with respect to the surface normal).

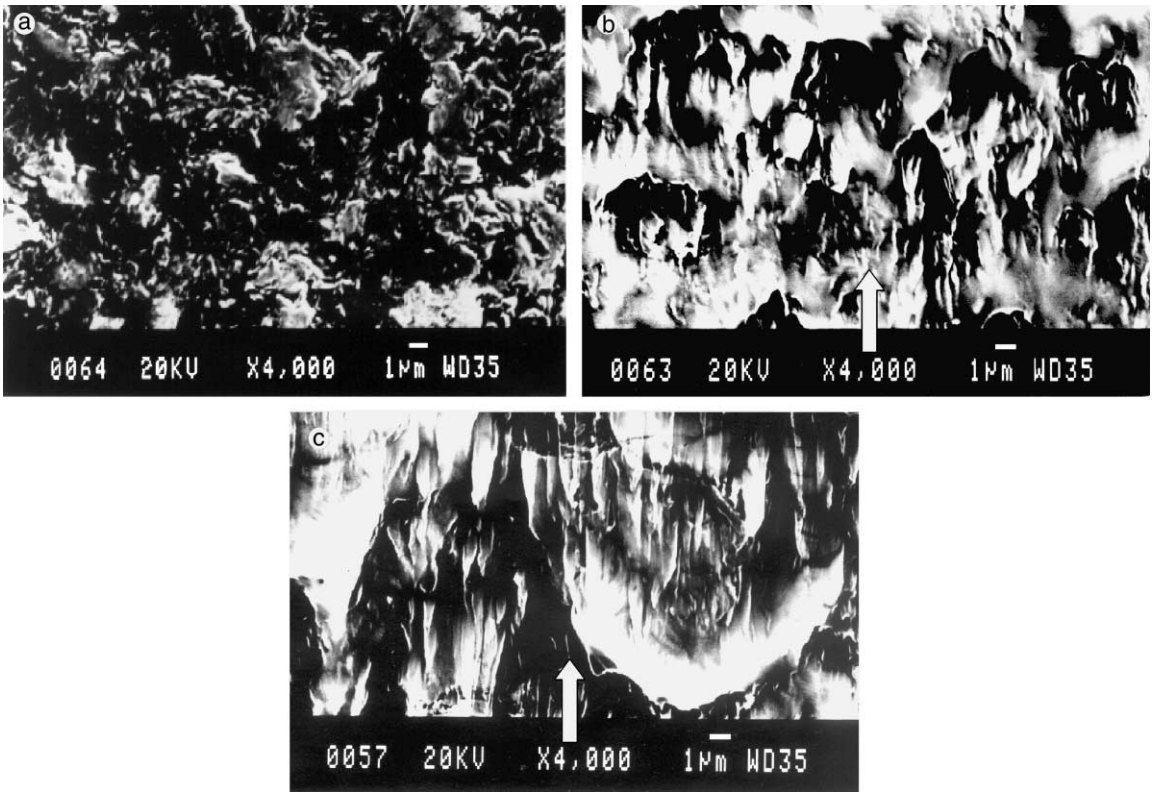

Fig. 2. SEM micrographs of graphite surfaces before (for POCO, a) and after 30 keV N_2^+ irradiation at $\theta = 60°$ (for POCO, b) and MPG-LT (c). The arrows show the ion beam direction.

Namely, the surface roughness increases, pore dimensions increase, protuberances between the pores (the column structures with cone-like tops) arise, and column axes coincide with the ion beam direction as the erosion theory predicts [25]. Typical images are presented in Fig. 2(b) and (c). The comparison of the results for the graphites investigated show, that the developed surface topography of POCO-AXF-5Q is slightly more smeared than that of MPG-LT. In particular, the lengths of the column structures for POCO are about a factor of two less than for MPG-LT. One may suppose that the discrepancies in the topography determine to a large extent the differences of the sputtering yields, Y (and also of γ) for MPG-LT and POCO, cf. [26–28]. Indeed, the sputtering yields for POCO-samples have been found more than 1.5 times higher than those for MPG-LT both at normal incidence and at oblique incidence. Only at $\theta = 60°$ the corresponding Y data are nearly the same, see Fig. 3. The density difference of MPG-LT and POCO cannot be the reason for the observed differences in the corresponding yields; according to the TRIM.SP simulations the dependence sputtering yields on density is negligible. At $\theta = 60°$ for $\rho = 1.85$ g/cm^3 the yield Y is 1.15, for $\rho = 1.7$ g/cm^3 it is $Y = 1.10$ at/ion.

In Fig. 3 the simulation data also presented in the case of graphite sputtering by 15 keV N [10]. The comparison with the experimental results shows that at oblique incidence the divergence with simulated data for POCO-samples is less than for MPG-LT. This may be due to a more smeared POCO surface topography. Namely, the presence of oblique surface structure elements results in a transformation of effective incidence angles relative to a smooth surface and it follows that at near normal incidence Y increases and at oblique ion incidence Y decreases in comparison with a ion incidence on smooth surface [26,27].

The comparison of γ for MPG-LT [24] and POCO shows, that is somewhat higher for POCO at oblique incidence than for MPG-LT, see Fig. 4. However, the difference is not so appreciable as in the sputtering case. One can also see, that in the angular range studied (0–80°) the angular dependence of γ is close to $\gamma = 4(\cos\theta)^{-0.7}$, i.e. this dependence is weaker than an inverse cosine dependence, which follows from the theoretical treatment for smooth surfaces [7].

The other reason of the discrepancies between the experiment and simulation in sputtering and between the experiment and theory in ion-induced electron

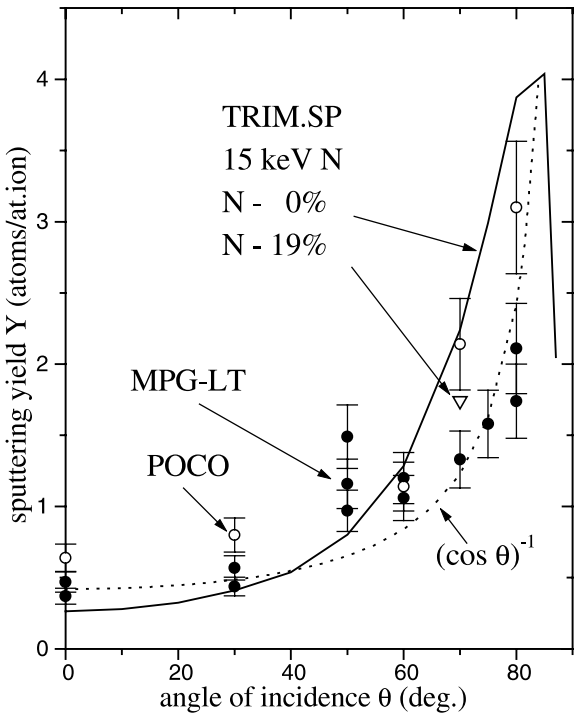

Fig. 3. The dependence of sputtering yields Y of graphites on ion incidence angle. Data for MPG-LT and simulation results for 15 keV N taken from [10]. (▽): simulation for C:N:O = 77:19:4.

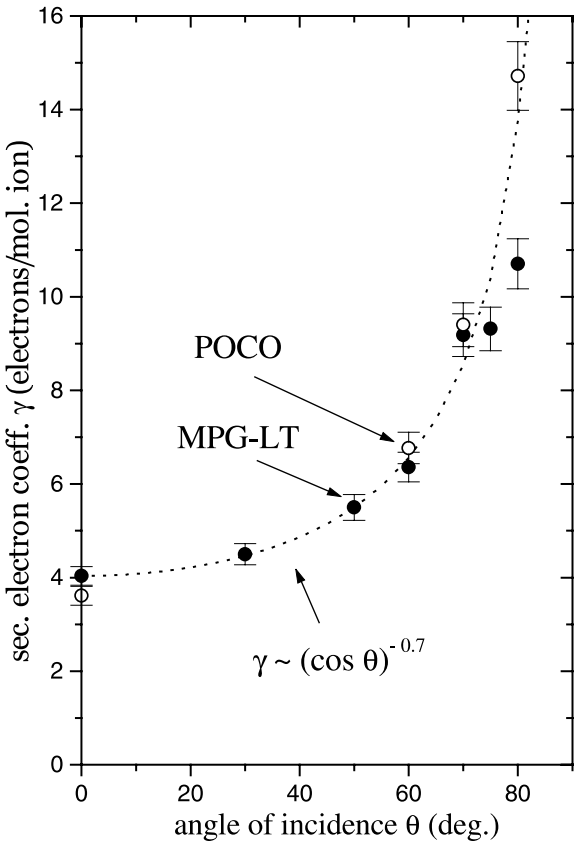

Fig. 4. The dependence of ion-induced electron emission γ on ion incidence angle θ under 30 keV N_2^+ ion bombardment. Data for MPG-LT are taken from [24].

emission may be connected with a modification of the graphite surface layer under ion implantation and the carbon-nitride compound formation [3–5]. The data of the elemental composition of irradiated graphites were obtained from the RBS spectra analysis. After high-dose irradiation at near room temperature nitrogen and oxygen were observed in the surface layers, see the corresponding peaks in the RBS-spectra presented in Fig. 5(a). Further experiments have shown, that the O-peak disappears at target temperatures $\geqslant 300$ °C.

The simulation of RBS spectra with the NBS program [18] has shown that the RBS-spectra are reasonably well described in the case of normal N_2^+ ion incidence on MPG-LT on the assumption, that the modified surface layer has the composition ratio C:N:O = 77:19:4 and a width of 54 nm. According to TRIM.SP simulations, this corresponds to full halfwidth of the distribution of 15 keV N in graphite. The implanted N concentration is about 16 at.% for POCO-AXF-5Q. It should be noted that comparable N concentrations in graphites under high-dose nitrogen implantation were observed in a number of studies. The N concentration was 25 at.% under 12 keV N_2^+ [4]: 22 at.% under 35 keV N^+ [29]; 18 at.% under 20–150 keV N^+ bombardment [30].

It has been found that the angular dependence of the N peak, h_N, in the RBS spectra is well described in a first approximation by a cosine dependence. This provides evidence, that the implanted N concentration at dynamically steady-state conditions is independent of the ion incidence angle. Typical data for MPG-LT are presented in Fig. 5(b). At the given experimental conditions, the steady-state N concentration is ≈20 at.% for MPG-LT and 16 at.% for POCO accordingly. Simulation of 15 keV N sputtering of graphite, taking into account the presence of implanted N in the modified layer, shows that ≈20 at.% of N decreases the carbon sputtering yield approximately by 20% in comparison with the yield if the implanted N is negligible. As an example in Fig. 3, the value of the carbon sputtering yield is $Y = 1.742$. The nitrogen and oxygen sputtering yields are 0.415 and 0.085, respectively.

The measured angular dependences of both Y and γ presented above were obtained at relatively low tem-

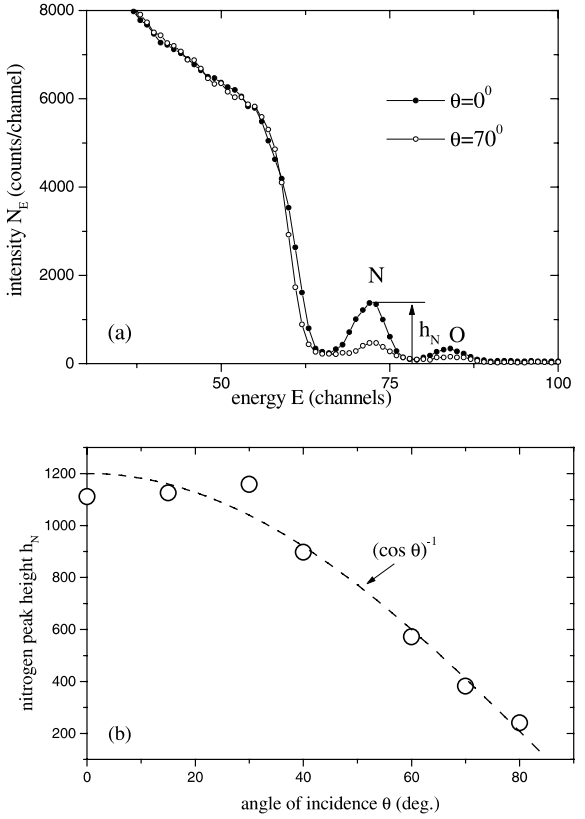

Fig. 5. RBS spectra of 1.7 MeV He^+ ions for MPG-LT after irradiation by 30 keV N_2^+ ions (a) and the dependence of the N-peak, h_N, on the angle of incidence, θ(b).

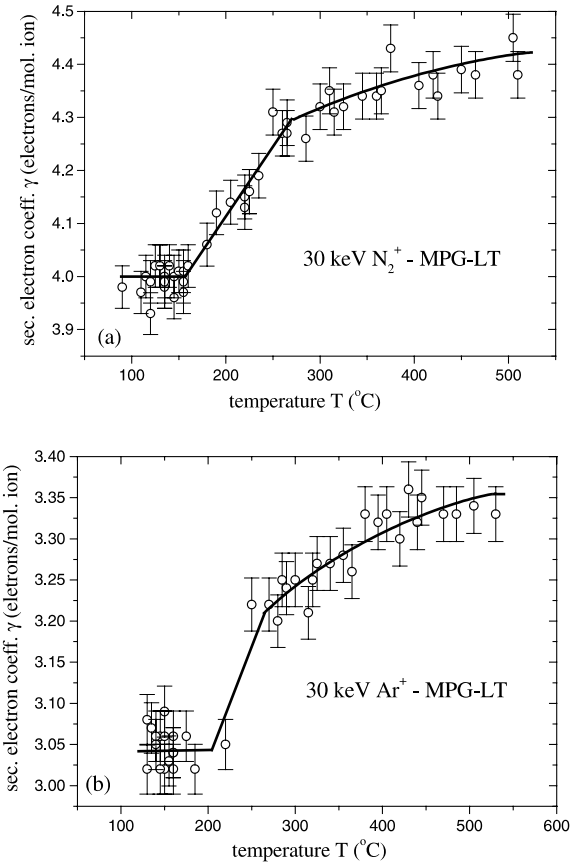

Fig. 6. The temperature dependences of γ for MPG-LT under 30 keV N_2^+ ion irradiation (a) and 30 keV Ar^+ ion irradiation (b) at normal incidence ($\theta = 0°$).

peratures ($\leqslant 60$ °C). It is known that damage pattern and many physical properties of ion irradiated carbon-based materials depend on the target temperature, see for example [31,32]. In particular, it was shown in [31] that the loss of crystallinity in graphites irradiated with 200 keV C^+ ions at 300 °C (observed from the comparison of the smearing degree of diffraction rings on RHEED patterns) at 300 °C is much less than after irradiation near room target temperature. One could expect that sputtering and ion-induced electron emission characteristics in the studied case would also depend on the temperature of the damage production. The measurements of γ in the target temperature range from 60 to 500 °C show that $\gamma(T)$ changes the slope at about 250 °C, indicating a different target behaviour above 250 °C. To control that this temperature behaviour of γ is not due to both the release of the implanted N or a carbon-nitride compound transformation the γ temperature dependence has been also measured at 30 keV Ar^+ ion bombardment. The temperature dependence of γ has been found analogous to the corresponding dependence for 30 keV N_2^+ bombardment, see Fig. 6(a) and (b).

5. Conclusion

Steady-state conditions of isotropic graphites (MPG-LT and POCO-AXF-5Q) during bombardment with nitrogen are characterized by the stabilization of the sputtering yield Y and the secondary electron coefficient γ; equilibrium of the implanted nitrogen concentration and a specific surface topography are reached at fluences of about 1×10^{19} N/cm^2 for 30 keV N_2^+.

The sputtering yields Y increase with the angle of incidence in the angular range investigated ($\theta = 0$–$80°$). For POCO-AXF-5Q the yields Y are about 1.5 times higher than for MPG-LT. The simulated angular dependence of the sputtering yield shows a maximum at $\theta \simeq 85°$. The discrepancies between experimental sputtering data and calculated values (TRIM.SP) may be a

consequence of both the developed surface topography and a modification of the surface layer composition by the high-dose nitrogen irradiation.

The implanted N concentration has been found to be about 20 at.% for MPG-LT and 16 at.% for POCO.

The increase with the angle of incidence of the ion-induced electron emission coefficient γ can be rather well described by $\gamma = 4(\cos\theta)^{-0.7}$ near room temperature.

The dependence of γ on the target temperature manifests a step-like increase at $\simeq$250 °C which may be due to a radiation induced structure transformation in the modified surface layer.

Acknowledgements

Research sponsored by the Ministry of Education of the Russian Federation, the Ministry of Science and Technologies of the Russian Federation (State contract no. 105-61(00)-P) and the Moscow Government (grant no. 2.1.24, 2000). The authors gratefully acknowledge very helpful discussions with A.E. Gorodetsky (Institute of Physical Chemistry of RAN, Moscow, Russia) and are grateful to V.G. Galstyn (Institute of Crystallography RAN, Moscow, Russia) for SEM analysis, to V.S. Kulikauskas for RBS analysis and to Alexey Nemov for help in the measurements.

References

[1] G. Federici, C.H. Skinner, J.N. Brooks, J.P. Coad, C. Grisolia, A.A. Haasz, A. Hassanein, V. Philipps, C.S. Pitcher, J. Roth, W.R. Wampler, D.G. Whyte, Plasma-Material Interactions in Current Tokamaks and their Implications for Next-Step Fusion Reactors, IPP-Report 9/128, 2001.
[2] D.L. Williamson, J.A. Davis, P.J. Wilbar, Surf. Coat. Technol. 103&104 (1998) 178.
[3] S. Muhl, J.M. Mendes, Diam. Relat. Mater. 8 (1999) 1808.
[4] F. Link, Y. Baumann, A. Markwitz, E.F. Krimmel, K. Bethge, Nucl. Instrum. Meth. B 113 (1996) 235.
[5] C. Palacio, C. Gomez-Aleixandre, D. Dias, M.M. Garcia, Vacuum 48 (1997) 709.
[6] H.H. Andersen, H. Bay, in: R. Behrisch (Ed.), Sputtering by Particle Bombardment I, Springer, Berlin, 1981.
[7] B.A. Brusilovsky, Appl. Phys. A 50 (1990) 111.
[8] R.A. Baragiola, in: J.W. Rabalais (Ed.), Low Energy Ion Surface Interaction, Wiley, New York, 1994, Ch. 4.
[9] W. Eckstein, Sputtering, Reflection and Range Value for Plasma Edge Codes, IPP-Report 9/117, 1998.
[10] A.M. Borisov, V.V. Zheleznov, V.S. Kulikauskas, E.S. Mashkova, W. Eckstein, Poverkhnost (5) (2001) 58 (in Russian).
[11] I.N. Evdokimov, E.S. Mashkova, V.A. Molchanov, Phys. Lett. 8 (1967) 619.
[12] I.N. Evdokimov, I.M. Fayazov, E.S. Mashkova, V.A. Molchanov, V.A. Snisar, Radiat. Eff. Defects Solids 112 (1990) 221.
[13] E.S. Mashkova, V.A. Molchanov, V.I. Shulga, C. Benazeth, N. Benazeth, P. Cafarelli, Eckstein, M. Hou, Nucl. Instrum. Meth. B 115 (1996) 519.
[14] Y. Kataoka, K. Wittmaack, Surf. Sci. 424 (1999) 299.
[15] E.S. Mashkova, V.A. Molchanov, Medium-Energy Ion Reflection from Solids, North-Holland, Amsterdam, 1985.
[16] E.S. Mashkova, V.A. Molchanov, I.M. Fayazov, W. Eckstein, Poverkhnost (2) (1994) 33 (in Russian).
[17] J. Bohdansky, C.D. Crossman, J. Linke, J.M. McDonald, D.H. Morse, A.E. Pontau, R.D. Watson, J.B. Whitley, D.M. Goebel, Y. Hirooka, K. Leung, R.W. Conn, J. Roth, W. Ottenberger, H.E. Kotzlowski, Nucl. Instrum. Meth. B 23 (1987) 527.
[18] A.M. Borisov, S.V. Luntzov, V.G. Sukharev, 7th Russian–Japanese International Symposium on Interaction of Fast Charged Particles with Solids, Program and Abstracts. 9–16 October 2000. Physico-Technical Research Institute of University of Nizhnii Novgorod, Nizhnii Novgorod, Russia, 2000, p. 56.
[19] W. Eckstein, Computer Simulation of Ion–Solid Interaction, Springer Series in Materials Science, vol. 10, Springer, Berlin, 1991.
[20] W. Eckstein, R. Dohmen, Nucl. Instrum. Meth. B 1291 (1997) 327.
[21] W.D. Wilson, L.G. Haggmark, J.P. Biersack, Nucl. Instrum. Meth. B 15 (1996) P.2458.
[22] J. Lindhard, M. Scharff, Phys. Rev. 124 (1961) 128.
[23] O.S. Oen, M.T. Robinson, Nucl. Instrum. Meth. 132 (1976) 647.
[24] A.M. Borisov, V.S. Kulikauskas, E.S. Mashkova, A.V. Safronov, Poverkhnost (8) (2001) 59 (in Russian).
[25] G. Carter, B. Navinsek, J.L. Whitton, in: R. Behrisch (Ed.), Sputtering by Particle Bombardment II, Springer, Berlin, 1983, Ch. 6.
[26] M. Kuestner, W. Eckstein, V. Dose, J. Roth, Nucl. Instrum. Meth. B 145 (1998) 320.
[27] J. Roth, W. Eckstein, E. Gauthier, J. Laszlo, J. Nucl. Mater. 779–781 (1991) 34.
[28] J. Mishler, B. Maurel, N. Benazeth, Radiat. Eff. Defects Solids 108 (1989) 145.
[29] E.A. Romanovsky, O.V. Bespalova, A.M. Borisov, N.G. Goryga, V.S. Kulikauskas, V.G. Sukharev, V.V. Zatekin, Nucl. Instrum. Meth. B 139 (1988) 355.
[30] J. Hartmann, A. Koniger, H. Huber, W. Ensinger, W. Assmann, B. Stritzker, B. Rauschenbach, Nucl. Instrum. Meth. B 117 (1986) 392.
[31] V.N. Chernikov, A.E. Gorodetsky, S.L. Kanashenko, A.P. Sakharov, W.R. Wampler, B.L. Doyle, J. Nucl. Mater. 220–222 (1995) 912.
[32] Y. Funada, K. Awazu, K. Shimamura, M. Iwaki, Surf. Coat. Technol. 103&104 (1998) 389.